USING REMOTELY-SENSED OBSERVATIONS TO DESCRIBE TROPICAL CYCLONE FORMATION AND EVOLUTION

13B.2

Miguel F. Pineros*
University of Arizona, Tucson, Arizona

1. Introduction

The interpretation of a tropical cyclone's structure from satellite imagery has been a key element for structure and intensity estimation. One of the most important examples is the Dvorak technique, which was developed in the 1970s, and is still used in many tropical cyclone forecasting centers (Dvorak 1975, 1984). This technique provides a source of tropical cyclone intensity estimates over the tropical oceans. The longevity of the Dvorak technique clearly speaks to the utility of satellite-based observations for tropical cyclone analysis. An aspect of tropical cyclone development that can clearly benefit from use of satellite-based observations is the genesis process. Tropical cyclones, for the most part, develop over oceans where traditional observation platforms such as rawinsonde stations cannot be located. Therefore, the best opportunity for locating and discriminating those cloud clusters that will develop into tropical cyclones from those that will not is from analysis of satellite-based observations.

This document introduces an objective technique, based on brightness temperature observations, which aims to characterize the structure and dynamics of tropical cyclones. The basis of the technique is that the convective structures embedded in cloud clusters become more axisymmetric as the wind field of the disturbance organizes and intensifies. To quantify this evolution, two tasks are required: 1) the center of the system needs to be located in an objective manner, and 2) the departure from axisymmetry of the weather system needs to be quantified. Time series of the combined results of these two tasks are used to examine the evolution of tropical disturbances, and it is shown that these time series are negatively correlated with the maximum sustained surface wind speed obtained from the National Hurricane Center best track archives.

The center location and axisymmetry quantification procedures are described in section 2. Results are presented in section 3, and finally, section 4 summarizes and presents conclusions.

2. Methodology

2.1. Data

The data used in this study are longwave infrared images from Geostationary Operational Environmental Satellite 12 (GOES-12). The first step in the process is to rectify these images from a natural earth coordinate system to a Cartesian projection removing much of the differences in pixel resolution due to the Earth's curvature. The resulting images are at a spatial resolution of 5 km/pixel and half-hourly temporal resolution.

2.2. Center Calculation

In this technique, the key element that is used to quantify the amount of axisymmetry and dynamics of a storm from an image is the gradient of the brightness temperature in the infrared images. These vectors indicate the direction of maximum change in the intensity; consequently their local organization can describe the structure of the shapes shown in

Corresponding Author Address: Miguel F. Pineros, University of Arizona. Department of Electrical and Computer Engineering, Tucson, AZ 85721. Email: mpineros@ece.arizona.edu.

the scene. After filtering the images to remove noise, the gradient is calculated by convolving the image with predefined templates (Gonzalez and Woods 2002). They provide vertical and horizontal derivatives required for the calculation of the gradient, and form the basis of the following procedures.

The next step in this technique is to identify a point which will be used to locate a circular area that encloses a weather disturbance in an image. The center location of this area is determined by projecting a line of 70 pixels length that is parallel to the gradient vector at each pixel across the domain. These results are accumulated in a matrix that initially contains zeros, each position where the projected line crosses in the image is incremented in the accumulator (or density) matrix. Consequently, a high number in the matrix indicates the position where a high number of lines intercept, since many gradient vectors are directed towards or away from that point. The locations of the maxima in the accumulator matrix are considered to be reference points or centers of the cloud systems in the image. One advantage of this technique is that the number of weather systems in the images does not need to be known in advance.

Figure 1 demostrates this procedure. An artificial image of an axisymmetric tropical cyclone that includes a cloud-free eye is shown in Figure 1a. In this case, all the gradient vectors are directed towards or away from the center of the image. Figure 1b Illustrates the gradient (blue vectors) of every pixel contained in the central square on Figure 1a, red lines correspond to the projections performed for two vectors indicated by the red arrows. Figure 1c shows the resulting matrix after accumulating these two projections. As an example of a real case, Figure 2 shows the accumulator matrix for an infrared image of Hurricane Beta (2005). The maximum in the accumulator matrix is indicated in red.

At early stages, a storm begins as a disorganized cloud cluster and generally becomes more axisymmetric as it intensifies. For this reason the maximum value in the accumulator matrix will increase as the storm intensifies, improving the confidence that the center or reference point of the weather system has been clearly identified.

2.3. Axisymmetry Quantification

The following task consists of characterizing the departure of the weather system structure from axisymmetry. This is performed by calculating the deviation angle of the brightness temperature gradient vector at each pixel with respect to a line connecting that pixel to the center (Figure 3a). Note that if the vector is aligned with the extended line, the departure angle is zero. This is the case of the ideal axisymmetric vortex shown in Figure 3b. This process is repeated for every pixel within 350 km of the reference point with the objective of building a distribution of deviation angles. An example of this result for the ideal vortex is shown in Figure 3c.

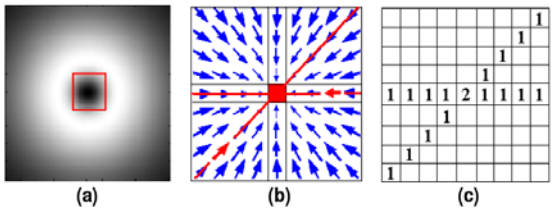

Figure 1. Example of the gradient line density calculation: a) brightness temperature image of an ideal vortex; b) gradient vectors of the ideal vortex's central section and the projected lines for two of its elements; and c) the resulting density matrix of the projected lines.

The variance of the deviation angle distribution corresponds to a measurement of the axisymmetry of the system around the reference point. In the case of the ideal axisymmetric vortex, the variance is zero. Conversely, disorganized clouds, not associated with a vortex, will be characterized by high variances due to the fact that the reference point is not well-defined and the gradient is extremely disordered.

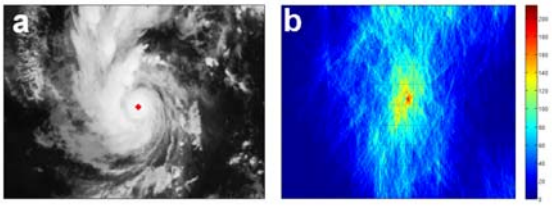

Figure 2. a) Infrared channel 4 (10.7 μm) image of Hurricane Beta at 0645 UTC October 30, 2005, estimated intensity: 100 kts; and b) the density matrix of the gradient projected lines for a).

Figure 4 shows three stages of the lifecycle of Hurricane Rita (2005), the reference point as calculated by the described procedure in section 2.2 is indicated in the images. Note that the variance in the distribution decreases as the storm increases in intensity until it becomes a well-structured vortex. Figure 5 illustrates three stages of a less intense system: Tropical storm Lee (2005). In this case, although the structures are very disorganized, the variance still decreases as the storm evolves.

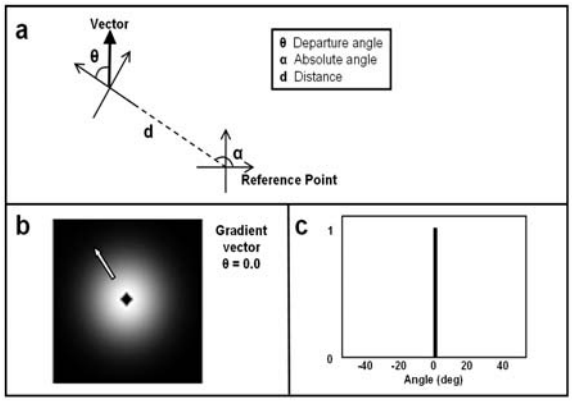

Figure 3. a) "Departure Angle" calculation. The reference point is the objectively-determined center of each object within the scene; b) example of the "departure angle" for an axisymmetric vortex; and c) histogram of departure angles for the ideal vortex in b).

3. Results

Approximately 9500 half-hourly longwave infrared images from GOES-12 during 2005 were processed. The input data contains 26 tropical cyclones: 2 tropical depressions, 11 tropical storms and 13 hurricanes, including average and rapid intensification periods, ocean-land paths, and cases from the tail end of this record-long season.

Time series of the deviation angle variance were generated for all 26 tropical cyclones and compared with the best track intensities produced by the National Hurricane Center. The temporal resolution of these two signals is different; therefore the best track intensity was linearly interpolated from 6h to half-hourly resolution to facilitate the comparison.

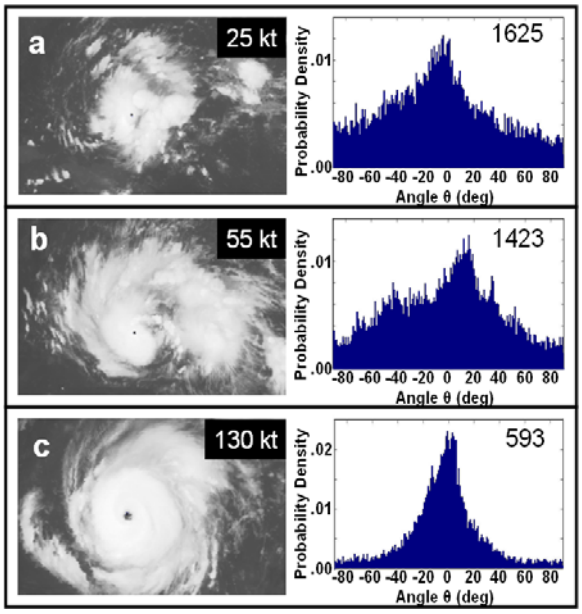

Figure 4. Sequence of infrared images and deviation angles distribution for Hurricane Rita (2005): a) 0815 UTC 18 September 2005. Intensity: 25kt, 1009 hPa,variance: 1625; b) 1415 UTC 19 September 2005. Intensity: 55 kt, 997 hPa, variance: 1423; and c) 1415 UTC September 2005. Intensity: 130kt, 932 hPa,variance: 593.

The deviation angle variance signal contains several frequency components. Some of them, especially the high frequencies, may be caused by a suboptimal location of the reference point, particularly at the early stages of the storm development when it is not well-defined. For the purposes of this study, each reference point in the image sequence was individually verified to

ensure that it was consistent from frame to frame.

Low frequency components in the deviation angle variance signal are those that best correlate with the interpolated NHC intensity estimates. Figure 6 shows the time series of the angle variance, low-pass filtered angle variance and the NHC wind speed estimates for Hurricane Rita (2005). In this case, the correlation calculated between the intensity and the variance is -0.85 and -0.9 for the unfiltered and filtered signals respectively. Recall that the angle variance decreases as the storm intensifies producing negative correlations.

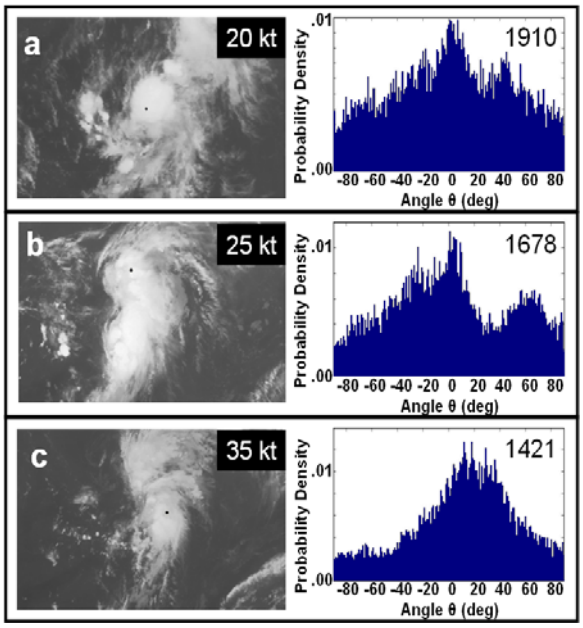

Figure 5. Sequence of infrared images and deviation angles histograms for Tropical Storm Lee (2005): a) 2115 UTC 29 August 2005. Intensity: 20 kt, 1009 hPa,variance: 1910 ; b) 0015 UTC 31 August 2007. Intensity 25 kt, 1010 hPa, variance: 1678; and c) 1615 UTC 31 August 2007. Intensity 35 kt, 1007 hPa,variance: 1421.

The average correlation magnitude over all 26 tropical cyclone cases is 0.74 on the filtered angle variance signal with the interpolated NHC intensity estimates. Figure 7 summarizes the results over all 26 cases. For 57% of the cases, the correlation magnitude is 0.8 or higher, the median is 0.83, and for those storms that reached hurricane strength the average correlation magnitude is 0.86. Only in four cases, Tropical storms Gert, Harvey, Jose and Alpha, had correlation magnitudes less than 0.5. In these cases the filtered variance signal contains high-amplitude fluctuations with 18-20h periods that diminish the correlation and overwhelm the intensity trend.

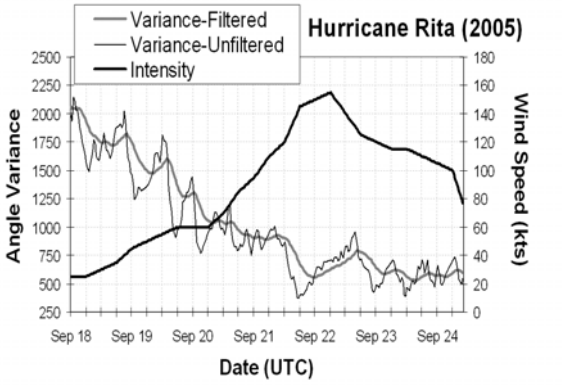

Figure 6. Time series of the best track intensity (kt) from the National Hurricane Center best track data (solid black), unfiltered angle variance (thin black; correlation:-0.85), and filtered angle variance (gray: correlation: -0.90) for Hurricane Rita.

Figure 8 shows the mean angle variance for all the analyzed storms against the NHC best track intensity estimates for periods of intensification only. The standard deviation about the mean value is shown by the errors bars, and the number of samples taken for each calculation is at the top of the figure. While there is small difference in the deviation angle variations calculated at these different values of intensity, the agreement is very good and indicates that the actual intensity estimate may be extracted from this signal.

4. Discussion and Conclusions

This paper describes an easily applicable and objective technique to measure the axisymmetry of a tropical cyclone around an identified reference point. It is based on the gradient of brightness temperature intensities in infrared

images; however it only relies on the direction of the vectors and not their magnitude and thus can characterize structures even when the intensity differences are small.

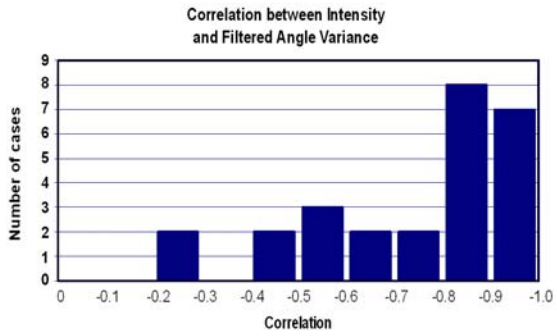

Figure 7. Histogram of the correlation values between the best track intensity and filtered angle variance for all 26 tropical cyclone cases. The mean correlation magnitude is 0.74, the median is 0.83, with a standard deviation of 0.23.

The deviation angle variance for each frame of IR imagery sequences signal is calculated to build a signal that is negatively correlated with the 30 min interpolated NHC best track intensity estimates. The correlation magnitude is remarkable for most of the cases: over 50% of them have a correlation of 0.8 of higher; the mean value is 0.74. These results indicate that the angle variance signal describes the evolution of dynamics of the system, and its values provide an estimate of the intensity of the tropical cyclone.

The fluctuations in the deviation angle signal can be caused by several factors that do not imply changes in the intensity: diurnal structure oscillations, the formation of mesoscale convective system with the tropical cyclone circulation, and suboptimal center calculation amongst other possibilities. Additionally, the performance of this technique is obtained by correlating the 30-min angle variance signal with the linearly interpolated NHC intensity estimates. Certainly that interpolation provides the intensity tendency but not fast and detailed changes. All of these factors diminish the average correlation and increases the error in the correspondence angle variance values to instantaneous intensity.

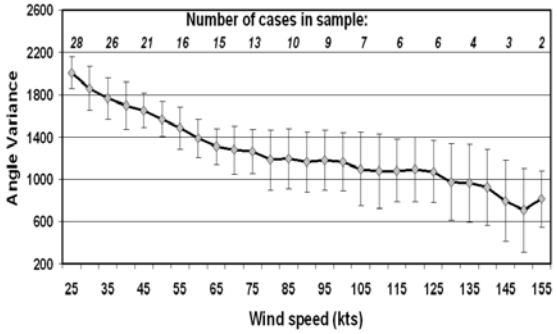

Figure 8. Average angle variance with one standard deviation error bars versus wind speed for all 26 tropical cyclone cases during intensifying periods. Note that there may be more than one time series for any given storm. The number of cases going into the mean and variance at each wind speed is indicated at the top of the graph in italics.

The technique shows potential to characterize the entire lifecycle of tropical cyclones from their earliest beginnings to their demise. Consequently, the technique is being enhanced to identify emerging tropical cyclones at early stages.

5. Acknowledgment

Author's advisors: Elizabeth A. Ritchie, University of Arizona. Department of Atmospheric Sciences, Tucson, AZ85721. ritchie@atmo.arizona.edu.

J. Scott Tyo. University of Arizona. College of Optical Sciences, Tucson, AZ 85721. tyo@optics.arizona.edu.

Best track data were obtained from the NOAA National Hurricane Center, FL website at http://www.nhc.noaa.gov. This research was supported by the Office of Naval Research under grant N00014-07-1-0185 and by the State of Arizona under a Technology and Research Initiative Fund Student Fellowship.

6. References

Dvorak, V. F. 1975: Tropical Cyclone Intensity Analysis and Forecasting from Satellite Imagery. Monthly Weather Review. 103. pp 420–430.

Dvorak, V. F. 1984: Tropical Cyclone Intensity Analysis Using Satellite Data. NOAA Technical Report NESDIS. 11, pp 45.

Gonzalez R.. Woods R, 2002: Digital Image Processing. 2nd Edition, pp 134.